Mercury speciation and Hg stable isotope ratios in sediments from Amazon floodplain lakes—Brazil

Beatriz Ferreira Araujo [iD],[1]* Holger Hintelmann,[2] Brian Dimock,[2] Rodrigo de Lima Sobrinho,[3] Marcelo Correa Bernardes,[3] Marcelo Gomes de Almeida,[1] Alex V. Krusche,[4] Thiago Pessanha Rangel,[1] Fabiano Thompson,[5] Carlos Eduardo de Rezende[1]*

[1]Laboratório de Ciências Ambientais, Centro de Biociências e Biotecnologia, Universidade Estadual do Norte Fluminense, Campos dos Goytacazes, Rio de Janeiro, Brazil
[2]Water Quality Centre, Trent University, Peterborough, Ontario, Canada
[3]Programa de Pós-Graduação em Geoquímica, Outeiro São João Baptista s/n Centro, Instituto de Química, Universidade Federal Fluminense, Niterói, Rio de Janeiro, Brazil
[4]Centro de Energia Nuclear na Agricultura, Universidade de São Paulo, Piracicaba, São Paulo, Brazil
[5]Centro de Ciências da Saúde, Instituto de Biologia, Universidade Federal do Rio de Janeiro, Rio de Janeiro, Rio de Janeiro, Brazil

Abstract

Hg concentrations and isotope ratios were measured to better characterize the mercury dynamics related to Hg cycling in Amazon floodplain lakes. We collected sediments, suspended particulate material (SPM), and plankton from floodplain lakes and compared then to sediments from rivers and soils of the central Amazon basin by measuring concentrations of total Hg (THg) and methylmercury (MMHg), and mercury isotope ratios. Concentrations of THg and MMHg in the lake sediments ranged to 69–109 ng g^{-1} and 0.62–4.78 ng g^{-1}, respectively. A positive correlation between THg and MMHg in soils and sediments suggest that inorganic Hg in this system is highly bioavailable and readily converted to MMHg. δ^{202}Hg values ranged from $-1.40‰$ to $-0.89‰$ and Δ^{199}Hg from $-0.34‰$ to $-0.18‰$. These values were comparable to those measured in riverine sediments ($-2.14‰$ to $-1.23‰$ and $-0.51‰$ to $-0.05‰$), suggesting a contribution of riverine sediments to lake sediments, at least during the season of rising waters, during which lake samples were collected. SPM on the other hand was much elevated in THg (590–1066 ng g^{-1}) and showed more negative δ^{202}Hg (-3.00 to -2.15), similar to those found in soils ($-2.99‰$ to $-2.17‰$), suggesting that Hg in SPM may originate from erosion of floodplain soils.

Every year, the Amazon River and its tributaries, which together drain the Amazon Basin, overflow and flood the adjacent land and forest, forming extensive wetlands. Large areas of standing water, called floodplain lakes, are formed from the river during the rainy season, which eventually drain into rivers in their respective sub-basins (Sioli 1984; Forsberg et al. 1988; Mertes et al. 1995). Approximately 44% of the area within the Amazon basin is subject to flooding by the Amazon River and its tributaries (Guyot et al. 2007).

This seasonal flood pulse, which is the driving force for river-floodplain systems responds to the rate of rise and fall of water (Junk et al. 1989). It creates distinct hydrological periods and inundates an extensive floodplain occupied by a complex mosaic of wetland habitats including alluvial forests, grasslands, and open water environments (Melack 1984). This process significantly affects hydrology, ecology, morphology, and geochemistry of these systems, and enables the regular exchange of a large amount of material between lentic and lotic ecosystems. It causes variations in thermal stratification, mixing dynamics, and affects a series of limnological parameters (e.g., pH, dissolved organic carbon [DOC], dissolved oxygen, and electric conductivity) that have a strong influence on the biogeochemistry of mercury (Melack and Fisher 1990; Roulet et al. 1998a; Guimarães et al. 2000; Brito et al. 2017). Lakes may continue to exchange water with the river through channels, even when water is receding and during droughts (Junk 1997).

Mercury (Hg) is recognized as a global pollutant due to its ability to be transported long distances from its original source, and its ubiquitous presence in aquatic ecosystems and food webs is an important environmental and human-health issue (Fitzgerald and Clarkson 1991). The form of mercury of greatest environmental concern is methylmercury (MMHg), as it is a highly potent neurotoxin which bioaccumulates in the

---

*Correspondence: bfaraujo@yahoo.com.br or crezende@uenf.br

Additional Supporting Information may be found in the online version of this article.

food chain (Morel et al. 1998). The high toxicity of mercury and its widespread distribution in the ecosystems are among the major environmental problems of the Amazon. The concern about Hg cycling in this ecosystem increased in the 1980s during the gold rush in the Brazilian Amazon (Guimarães et al. 2000). High mercury levels were found in different compartments, attributed mainly to gold mining activities (Pfeiffer et al. 1993; Malm 1998; Akagi and Naganuma 2000). Some authors later suggested that Amazon soils have high natural mercury concentrations that could explain the Hg values measured in the region (Roulet and Lucotte 1995; Wasserman et al. 2003). Other authors hypothesized that the atmospheric transport of anthropogenic mercury could be responsible for the widespread contamination of the Amazon basin (Lacerda 1995; Roulet et al. 1998*b*). As well, cattle farming and agriculture resulted in continued deforestation since the early 1970s, increasing soil erosion and probably contributing directly (and indirectly) to mercury dispersion (Hacon et al. 2008; Oestreicher et al. 2017). Consequently, the mercury cycling within the Amazon basin is likely affected by both natural and anthropogenic sources. Despite all of this information, sources of Hg in the Amazon are still a subject of great debate, complicated by the large natural variation in background mercury concentrations and/or large-scale transport of mercury throughout the region (Lechler et al. 2000).

In this context, the use of Hg stable isotope ratio measurements may offer new insight into the biogeochemical cycling of Hg (Yin et al. 2014). Mercury has seven natural stable isotopes: ^{196}Hg (0.15%), ^{198}Hg (9.97%), ^{199}Hg (16.87%), ^{200}Hg (23.10%), ^{201}Hg (13.18%), ^{202}Hg (29.86%), and ^{204}Hg (6.87%) of which six are sufficiently abundant (7–30%) for precise measurement of isotope ratios (Blum and Bergquist 2007). As long as different Hg sources are isotopically distinct, Hg isotope ratio measurements may allow source attribution or source tracing of Hg (Carignan et al. 2009; Feng et al. 2010; Perrot et al. 2010; Das et al. 2015). Mercury also has active redox chemistry, a volatile form (Hg^0), and a tendency to form covalent bonds. In the environment, mercury is subject to a variety of chemical, physical, and biological processes, which may result in both mass dependent fractionation (MDF) and mass independent fractionation (MIF) (Run-Sheng et al. 2010), both of which have been used to better understand the processes controlling Hg transport, transformation, and bioaccumulation (Blum et al. 2014). A major challenge in source apportionment studies of Hg is the identification and quantification of different sources once Hg has been dispersed and intermixed in the environment (Lindberg et al. 2007). However, anthropogenic sources of Hg to the environment frequently have distinguishable isotopic signatures, allowing Hg from those sources to be traced. Both mass-dependent (represented as δ^{202}Hg) and mass-independent fractionation (represented as Δ^{199}Hg) varies significantly among different source materials (Balogh et al. 2015) and can be used to either constrain the contamination sources in sediments (Foucher

and Hintelmann 2009; Feng et al. 2010; Perrot et al. 2010; Sonke et al. 2010) or the processes that Hg was subjected to in the atmosphere (Carignan et al. 2009; Rolison et al. 2013) and in the water column (Sherman and Blum 2013; Balogh et al. 2015; Yin et al. 2015; Zheng et al. 2015) prior to deposition into sediment.

Thus, characterizing the Hg isotopic ratios in aquatic systems may be an important tool to better understand the mobility, toxicity, transformation, and biogeochemical cycle of Hg in such ecosystems (Chen et al. 2010). Analyzing the spatial and temporal variations of Hg isotopic ratios in the environment and linking it to isotope fractionation caused by natural processes and human activities can provide valuable information about sources and biogeochemical cycling of the Hg (Jackson et al. 2008).

The main goal of our study is to better characterize mercury in dynamics in surface sediments of Amazon floodplain lakes. Specifically, we employed Hg isotope ratio measurements to gain a better understanding of the relationship between Hg in soils, river, and lake sediments. In concert with other geochemical parameters including species concentration, it is a first attempt to shed more light on Hg cycling in this area and to possibly characterize the movement of Hg through the various compartments.

Materials and methods

Study site

The Amazon basin covers an area of 6.3×10^6 km^2 and extends over eight South American countries, with 63% of this area being in Brazil (Salati and Vose 1984). It is the largest river system on the globe, interlaced by numerous large and small rivers (Goulding et al. 2003). The length of the Amazon was estimated to be ca. 7000 km, and the river is up to 5 km wide just below the mouth of the Negro River (Sioli 1984). The mean annual discharge is 200×10^3 m^3 s^{-1} at Óbidos, the most downstream gaging station in the Amazon River (Callede et al. 2000). Rivers within the Amazon drainage basin are traditionally classified according to water color, as well as physical and chemical parameters and are categorized as white (e.g., Solimões, Madeira, and Amazon), that have a near neutral pH and are enriched in dissolved major cations and in suspended particles (from 60 mg L^{-1} to 200 mg L^{-1}) eroded from the Andean cordillera; black (e.g., Negro) that drain forested areas, are characterized by high concentrations of DOC (7–10 mg L^{-1}), low contents in total major cations and in suspended particles (< 10 mg L^{-1}) and a pH varying from 4 to 5; or clear water (e.g., Tapajós) which present a slightly green to transparent coloration, an alkaline pH, and poor mineral and nutrient contents. (Sioli 1984; Maia et al. 2009).

In the central Amazon basin, the river is characterized by an annual monomodal fluctuation in water levels of about 10 m between high water and low water seasons (Junk et al. 1989). The amount of water on the various Amazon floodplains and
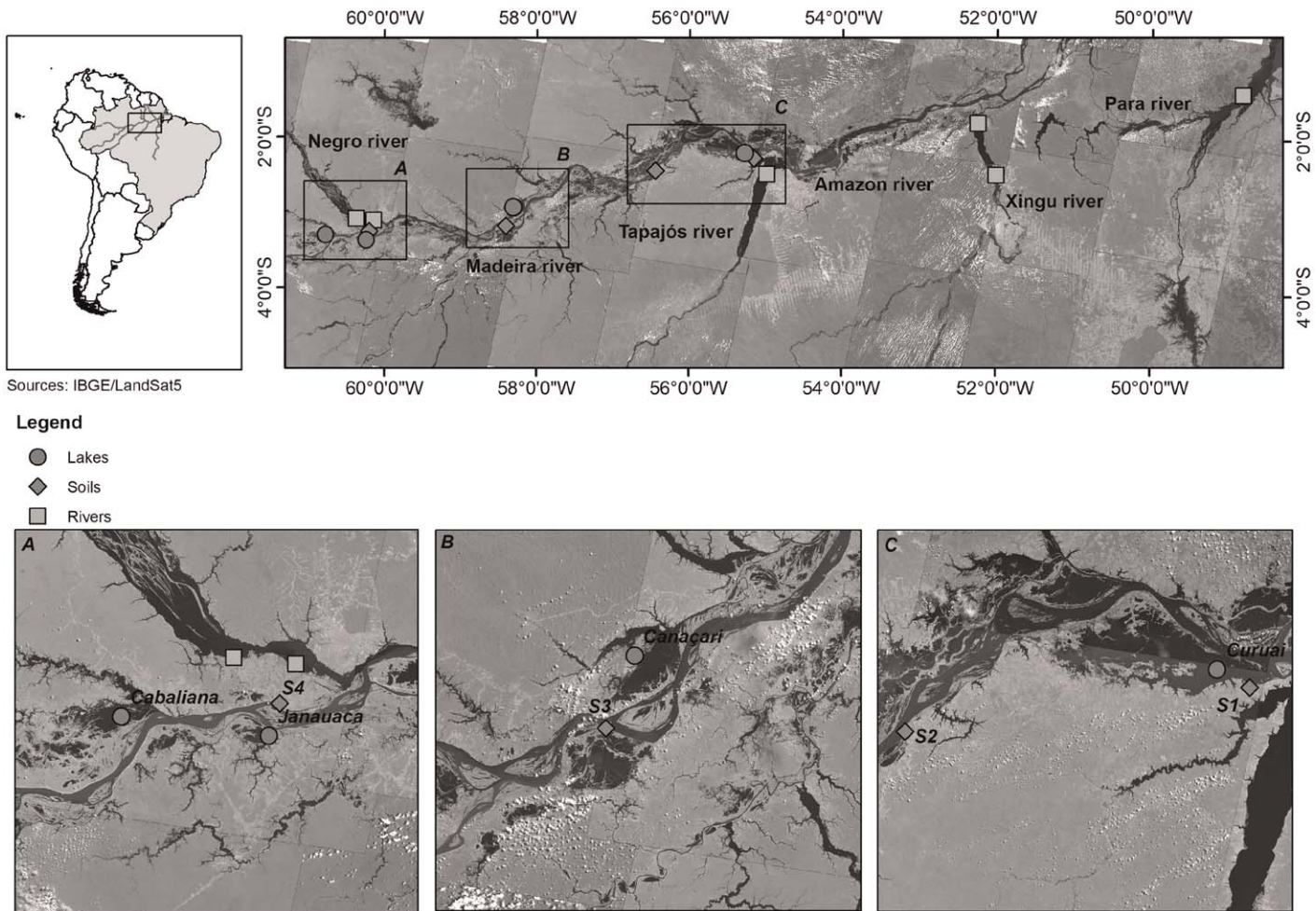
Fig. 1. Sampling locations for sediments, soils, and suspended particulate material in the Amazon Basin.

the amount exchanged with river channels is essential for understanding sediment delivery and nutrient exchanges that occur between the rivers and their floodplains (Dunne et al. 1998). These floodplain lakes have a complex hydrology, characterized by periodic flooding and aquatic interfaces between creeks and the main river (Melack 1984; Junk 1997). Two extreme seasons can be classified with high waters during the period from May to July, when the river flow is at its maximum and low waters with minimal flow of water between the months of October and November. The period of heavy frequent rainfalls and increasing river water levels is in the months from December to April, while the dryer period between high and low water seasons is in the months of August and September (Sioli 1984).

The floodplain lakes are located along the Solimões-Amazon river shoreline in a biogeographic gradient of upstream flooded forests to downstream flooded woodlands and open water lakes (Abril et al. 2014) (Fig. 1). Cabaliana is a round lake surrounded by flooded forests and associated with two subregions. In the northern region, the Manacapuru River

discharges clear water while in the southern region, white water brought by the Solimões River mixes with clear water. Janauaca has a peculiar morphology with a ravine shape surrounded by flooded forests. Solimões water arrives through the channel in the north and clear water through a stream system in the south. This lake reaches a peak flooded area of 180 km² at high water. Canaçari has two well-defined subregions. In the northern region, the Urubu River discharges black water and in the southern region, the Amazon River discharges white water. It is surrounded by flooded forests and woodlands. Curuai is the largest lake in the central Amazon basin, mainly surrounded by woodlands and open waters. It receives white water from the Amazon River through small channels, apart from the main channel in the eastern side. There are small contributions of black water streams in its most southeastern part (Table 1).

Sampling

Surface (0–2 cm) sediment samples were collected in the center of the lakes using a grab Van Veen grab sampler in

Table 1. Geomorphological and hydrological characteristics of the four floodplain lakes.

	Cabaliana	Januaca	Canaçari	Curuai
Latitude (S)	3° 18′46″	3° 23′20″	2° 58′60″	2° 09′44″
Longitude (W)	60° 40′15″	60° 16′26″	58° 15′40″	55° 27′53″
Shape	Ellipsoid	Ravine/dendritic	Ellipsoid	Triangular
Shoreline	Forests	Forests	Forests/woodlands	Woodlands/shrub
Water	Black/mixed	Black/mixed	Black/mixed	White
Conductivity (μS)	10–80	33–71	10–54	41–69
Temperature (°C)	28–34	29–33	29–34	30–36

Cabaliana, Janauaca, Canaçari, and Curuai lakes in the central Amazon basin between Manaus and Santarém (Fig. 1). Samples were collected between January 2011 and February 2011 to represent the raining season (rising water [RW]).

Additionally, nonflooded soils ("terra firme" soils) and river sediments samples were collected during the dry season (low water). Four superficial soil samples were collected in the Amazon River margin between Canaçari and Curuai in October 2009, and riverine sediments samples collected in the middle of the Negro, Tapajós, Xingu, and Pará rivers between September 2011 and November 2011. At each location, two dredged samples of approximately 5 g of surface layer were taken from the top 2 cm. On the ship, samples were stored and transported frozen (−20°C) to the lab, where they were immediately freeze-dried (−50°C for 72 h).

All soils samples were manually collected using stainless steel spatulas. After sampling, sediment and soils were stored in acid washed plastic bottles with screw caps. The duplicates were homogenized and crushed prior to chemical analysis.

Suspended particulate material (SPM) samples were collected in the four floodplain lakes (Cabaliana, Janauaca, Canaçari, and Curuai) (Fig. 1). To determine SPM concentrations, 500 mL of water was filtered using ashed (overnight at 450°C) and pre-weighed glass-fiber filters (Whatman GF-F, 0.7 mm, 47 mm diameter). Plankton samples were collected at the same sampling sites, where SPM was sampled. Conical plankton nets (1 m diameter) were hauled horizontally approximately 1 m below the water surface for about 5 min to avoid the capture of drifting living organisms or coarse particulate matter. Samples collected with 64 μm net were considered as zooplankton. Since the classification was based on the mesh size of the nets, some algae were probably present in the zooplankton samples.

Geochemical measurements

Organic matter (OM) in the floodplain lakes of the central Amazon basin may potentially be derived from: (1) terrestrial Andean clay-bound and refractory suspended particulate OM, which may be transferred to the floodplain lakes via the Solimões-Amazon and Madeira rivers; (2) nonflooded soils and litters of the Amazonian lowland forests (nonflooded forests), which is transferred to the floodplain lakes via local streams; (3) wetland soils (flooded forests) and litters (leaves, grasses, woods,

etc.), transferred to the floodplain lakes during the receding waters (falling water season) or the rainy season (RW season); (4) wetland aquatic and semi-aquatic macrophyte vegetation of the floodplain lakes; and (5) phytoplankton from the river or produced in the lake itself (Sobrinho et al. 2016).

Organic carbon (OC) and stable carbon isotope ratios were measured using a Flash 2000 organic elemental analyzer interfaced with a Delta V advantage isotope ratio mass spectrometer at the *Laboratório de Ciências Ambientais* (*Universiade Estadual do Norte Fluminense*—Rio de Janeiro—Brazil). The average precision was ± 0.1 mg C g^{-1} for Total Carbon. δ^{13}C values were calculated and reported in the standard delta notation relative to Vienna Pee Dee Belemnite (VPDB) standard. The analytical precision (as the standard deviation for repeated measurements of the internal standards) was ± 0.06‰ for δ^{13}C.

Mercury and monomethylmercury concentration

To avoid contamination by Hg, all materials and equipment was subjected to a rigorous cleaning protocol. Moreover, all unbagged equipment was handled with gloved hands in dedicated clean areas, including countertops covered by Teflon overlays within a Hg-free laminar flow-hood. To determine the concentrations of total Hg (THg), samples of approximately 0.5 g (dry weight) were digested with a $HNO_3 : H_2SO_4$ (7 : 3) mixture by gradually heating from 40°C to 200°C over a period of no less than 3 h. Acid digests were then cooled and brought up to a final volume of 20 mL. Sample digests were analyzed for THg by cold-vapor atomic fluorescence spectrometry (CVAFS, Tekran 2600) based on EPA Method 1631 (US EPA 1631 1999). Monomethylmercury (MMHg) was isolated by distillation, followed by atomic fluorescence spectrometry coupled with gas chromatography measurement (Tekran 2700) system based on EPA method 1630 (US EPA 1630 1998). THg and MMHg determinations of certified reference materials (NIST SRM 1944 and IAEA-405) were within 90–110% and 80–95% of the certified valued, respectively, and coefficients of variation of triplicate analyses were < 10%.

Mercury isotope ratio measurements

Hg isotope ratios were determined by multicollector inductively coupled plasma mass spectrometry (Neptune, Thermo-Fisher, Germany) at the Water Quality Centre (WQC) at Trent

Table 2. TOC and δ^{13}C values for the four floodplain lakes.

		OC (%)	δ^{13}C (‰)
Floodplain lakes	Cabaliana	3.5	−32.9
	Janauaca	1.5	−31.2
	Canaçari	2.5	−29.9
	Curuai	2.3	−27.9
Amazon rivers	Negro river 1	3.5	−29.0
	Negro river 2	3.2	−29.3
	Tapajós river	3.2	−30.3
	Xingu river 1	4.3	−28.5
	Xingu river 2	3.4	−29.2
	Para river	0.3	−30.3
Soils	S1	2.3	−30.3
	S2	2.1	−29.1
	S3	4.2	−27.4
	S4	4.3	−28.7

University. Sample solutions (Hg concentrations varied from 0.5 ng mL^{-1} to 2 ng mL^{-1}) were analyzed using a continuous flow cold vapor generation system with stannous chloride reduction (Foucher and Hintelmann 2006). The Faraday cups were positioned to measure five Hg isotopes (^{198}Hg, ^{199}Hg, ^{200}Hg, ^{201}Hg, ^{202}Hg). MDF of Hg isotopes was expressed using the delta notation (δ^xHg, in ‰) as defined:

$$\delta^x\text{Hg}(‰) = \{(\delta^x\text{Hg}/\delta^{198}\text{Hg})_{\text{sample}}/(\delta^x\text{Hg}/\delta^{198}\text{Hg})_{\text{standard}} - 1\} \times 1000 \tag{1}$$

Where $x = 199, 200, 201, 202$, "standard" represents the NIST SRM 3133 Hg solution. MIF of both odd and even Hg isotopes was defined by the deviation from the theoretically predicted MDF and expressed as (in ‰):

$$\Delta^{199}\text{Hg} = \delta^{199}\text{Hg} - 0.252 \times \delta^{202}\text{Hg} \tag{2}$$

$$\Delta^{200}\text{Hg} = \delta^{200}\text{Hg} - 0.502 \times \delta^{202}\text{Hg} \tag{3}$$

$$\Delta^{201}\text{Hg} = \delta^{201}\text{Hg} - 0.752 \times \delta^{202}\text{Hg} \tag{4}$$

Reproducibility of the isotopic data was assessed by measuring replicate sample digests every 10 samples. We also analyzed a UM-Almadén solution as a secondary standard in addition to the bracketing NIST 3133 standard solution. Our repeated measurements of UM-Almadén Hg gave long-term ($n = 24$) average δ^{202}Hg and Δ^{199}Hg values of -0.48 ± 0.16‰ and -0.02 ± 0.05‰, respectively, consistent with previously reported values (Blum and Bergquist 2007).

Statistical tests

To evaluate the differences among different matrices, the nonparametric Kruskal–Wallis and a post hoc test least significant difference were used. Groups that showed significant differences ($p < 0.05$) were assigned with different letters. The statistical test was performed with the software Statistic program 8.0 (StatSoft). The criterion for significance was $p < 0.05$.

Results

OC content and stable isotopic composition

The total organic carbon (TOC) and δ^{13}C values measured in the floodplain lakes ranged from 1.5% to 3.5% and -32.9‰ to -27.9‰. The TOC in river sediments and soils varied from 1.6% to 4.3% and δ^{13}C from -30.3‰ to -27.4‰, respectively (Table 2). No significant differences were observed between lakes and rivers and lakes and soils for both parameters (Supporting Information Material 1). The OC content was lowest in the downstream Lake Janauaca and the highest in Lake Cabaliana (Table 2). Similarly, δ^{13}C values were significantly less negative (by approximately 3‰) in the downstream lakes.

Concentrations of THg and monomethylmercury and Hg isotope ratios

THg and MMHg concentrations obtained in the lake sediments varied from 69 ng g^{-1} to 109 ng g^{-1}, and 0.62 ng g^{-1} to 4.78 ng g^{-1}, respectively. The sediments showed negative δ^{202}Hg ranging from -1.40‰ to -0.89‰ (mean: -1.14 ± 0.22‰) and Δ^{199}Hg values ranged from -0.34‰ to -0.18‰ (mean: -0.28 ± 0.08‰) (Table 3).

THg and MMHg values for river sediments ranged from 36 ng g^{-1} to 1025 ng g^{-1} and 0.30 ng g^{-1} to 26.1 ng g^{-1}, respectively. THg concentrations in soils varied from 19 ng g^{-1} to 68 ng g^{-1} and MMHg ranged from 0.51 ng g^{-1} to 1.01 ng g^{-1}. Hg isotope ratios in river sediments ranged from -2.14‰ to -1.23‰ (mean: -1.58 ± 0.17‰) for δ^{202}Hg and -0.51‰ to -0.05‰ (mean: -0.28 ± 0.17‰) for Δ^{199}Hg. Finally, soil samples showed δ^{202}Hg values ranging between -2.17‰ and -2.99‰ (mean: -2.60 ± 0.34‰). Δ^{199}Hg varied from -0.63‰ to -0.14‰ (-0.38 ± 0.22‰) (Table 3).

The THg, δ^{202}Hg, and Δ^{199}Hg averages values for SPM was 779 ng g^{-1}, -2.60‰, and -0.49‰ and was for plankton net (64) was 411 ng g^{-1}, -0.78‰, and -0.28‰, respectively (Table 3).

Discussion

OC content and stable carbon isotope composition

The δ^{13}C values steadily increase in lake sediments in a downstream direction. Due to the absence of random variations, we propose that a single overriding mechanism may be responsible for the observed trend. Most likely, an increased contribution of C$_4$ macrophytes to the soil OM is responsible for the progressively less negative values (Sobrinho et al. 2016).This explanation would be supported by other studies in the central Amazon basin, which reported that the abundance of macrophytes in this lakes increases in open water lakes and floodplains (Victoria et al. 1992; Martinelli et al. 2003; Sobrinho et al. 2016).

Table 3. Concentrations of THg and MMHg, and mercury isotope ratios in sediments, soils, and suspended material from the Amazon Basin.

	Location	Sample	THg (ng g^{-1})	MMHg (ng g^{-1})	δ^{202}Hg (‰)	Δ^{199}Hg (‰)	Δ^{200}Hg (‰)	Δ^{201}Hg (‰)
Floodplain lakes	Cabaliana	Sediment	109	3.6	−1.02	−0.36	−0.11	−0.19
		Net (64)	—	—	—	—	—	—
		SPM	590	—	−2.15	−0.59	−0.32	0.28
	Janauaca	Sediment	90	4.8	−0.89	−0.24	0.02	−0.19
		Net (64)	304	—	−2.25	−0.05	0.05	−0.07
		SPM	826	—	−2.9	−0.32	−0.10	−0.04
	Canaçari	Sediment	69	0.62	−1.25	−0.34	−0.02	−0.35
		Net (64)	827	—	0.74	−0.15	−0.07	−0.17
		SPM	1066	—	−2.37	−0.78	−0.34	−0.35
	Curuai	Sediment	76	2.5	−1.40	−0.18	−0.04	−0.11
		Net (64)	107	—	−0.82	−0.62	−0.36	−0.33
		SPM	633	—	−3.00	−0.26	−0.32	0.02
Amazon rivers	Negro 1	Sediment	208	0.15	−1.55	−0.51	0.02	−0.45
	Negro 2		169	0.24	−1.71	−0.43	−0.05	−0.37
	Tapajós		759	19.3	−2.14	−0.35	−0.07	−0.33
	Xingu 1		1025	25.6	−1.46	−0.05	0.00	−0.09
	Xingu 2		854	26.1	−1.23	−0.15	−0.03	−0.37
	Para		36	0.30	−1.39	−0.19	−0.1	−0.57
Soils	S1	—	20	0.51	−2.17	−0.5	−0.03	−0.49
	S2	—	39	0.79	−2.99	−0.63	−0.15	−0.59
	S3	—	68	1.01	−2.66	−0.27	−0.21	−0.15
	S4	—	19	0.68	−2.58	−0.14	−0.02	−0.01

THg and monomethylmercury concentrations

Hg species concentrations in lake sediments presented no significant difference when compared to soils and riverine sediments (Supporting Information Material 1). We suggest that the mercury concentrations observed in the floodplain lakes during January/February may reflect the flood pulse associated with RWs. This season is characterized mainly by two processes, resuspension of bottom sediments and erosion of river banks (Meade et al. 1979), which results in mercury leaching from adjacent soils and downstream transported to the floodplain (Roulet et al. 1999; Maia et al. 2009). The important role of rivers in exporting Hg to the floodplain lakes, this influence has been reported in the Curuai by the Amazon river (Maia et al. 2009) and in the Januaca by the Solimões River (Brito et al. 2017). Atmospheric deposition maybe an additional source of Hg to the floodplain lakes. A study conducted in sediments from Puruzinho Lake (Madeira River Basin) during wet seasonal period observed THg concentrations ranging from 44 ng g^{-1} to 129 ng g^{-1} (Almeida et al. 2014). The authors concluded that the distribution of Hg is mainly controlled by an import of Madeira river water during flooding, while the predominant process in the dry season was the remobilization of THg due to the resuspension of bottom sediments (Almeida et al. 2014).

THg concentrations in SPM were significantly different compared to lake sediments and plankton, presenting considerably higher average concentrations (779 ng g^{-1}) (Table 3). Similarly, in a study of Curuai Lake, Maia et al. (2009) found large variations of THg in SPM ranging from 42 ng g^{-1} to 1860 ng g^{-1} during the flooding period. According to the authors, Hg in white water lakes is mainly transported in its particulate phase during sediment and water exchange in the river and connected lakes. Moreover, the authors observed that the water column experiences a significant input of particulate Hg from bottom sediments during the dry season (October–November), caused by the resuspension of bottom sediments by wind and bioturbation. On the other hand, they highlighted that most of the Hg in remote soils and sediments of black water lakes is supplied by atmospheric deposition. Our results are also in agreement with those reported by Roulet et al. (1998c) for the Pacoval Lake along the Amazon River (139–411 ng g^{-1}).

The high THg concentrations found in plankton may suggest that Hg is taken up effectively into the lower food chain. In fact, the plankton community, which represents the first link in the aquatic food chain, plays a key role in the bioconcentration and biomagnifications of mercury. Phytoplankton incorporates mercury by adsorption and absorption of dissolved mercury species, while zooplankton
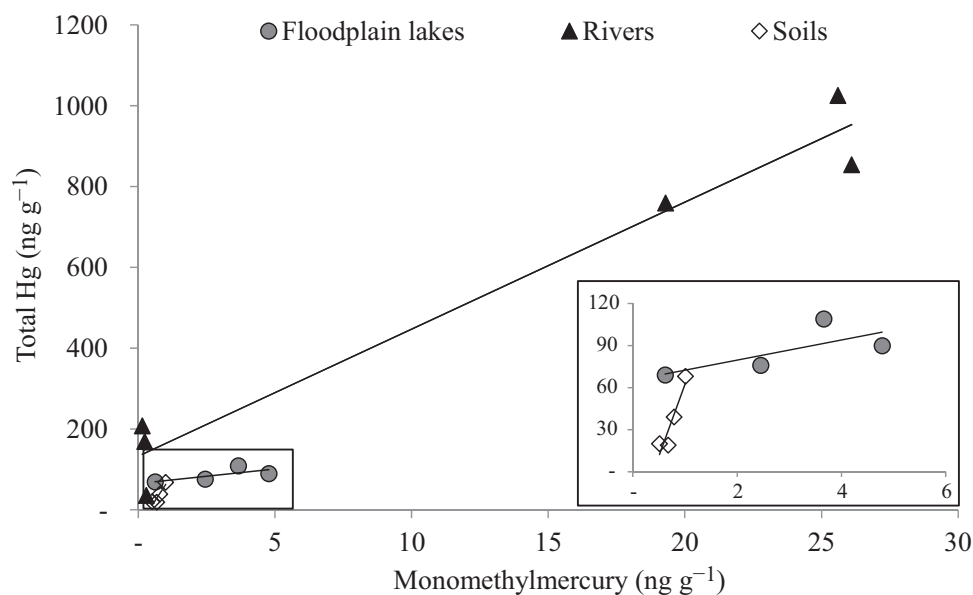
Fig. 2. Relationship between THg and MMHg in the sediments from the Amazon floodplains, riverine sediments, and soils.

incorporates mercury by ingestion of contaminated algae, suspended particulate matter (organic and inorganic detritrus), other zooplankton, and bacteria or by direct absorption from water (Tsui and Wang 2004; Brito et al. 2017). According to Brito et al. (2017), plankton biomass and the level of contamination of the surrounding environment are thought to be the key factors controlling the concentrations of Hg in plankton and the aquatic food web in general.

The MMHg concentrations observed in the lakes sediments represents less than 10% of the THg. No significant differences were observed among lake sediments, soils, and riverine sediments (Supporting Information Material 1). When deposited, inorganic mercury is incorporated into sediments rich in allochthonous OM, may be converted into MMHg under anaerobic conditions, and is subsequently accumulated by detritivorous organisms and biomagnified in the food chain (Ullrich et al. 2001). The black waterbodies, especially at the beginning of the rainy season, offer conditions for the methylation process, mainly due to the presence of labile OM. On the other hand, their dark color may shield MMHg from intense solar radiation, which otherwise could initiate its photodegradation (Bisinoti and Jardim 2004; Silva et al. 2009).

A study with sediments from Lake Piranga (Tapajós Basin), showed that the flooding had a clear effect on Hg methylation at the surface of semi-aquatic shoreline sediments (macrophyte zone) and semi-terrestrial forest soils, where MMHg concentrations and burdens appeared to be three times higher immediately following inundation (Roulet et al. 2001). In the Tapajos River floodplain, Guimarães et al. (2000) observed much higher (by a factor of 30x) Hg-methylation rates in the periphyton of adventive roots of

aquatic macrophytes compared to those found in adjacent sediments. Considering that macrophytes represent approximately 60% of the total carbon production in floodplain systems, it clearly makes them an important source of MMHg for the aquatic food chain.

A significant correlation was observed between THg and MMHg in lake sediments (0.979, $p < 0.05$, $n = 4$), riverine sediments (0.724, $p < 0.05$, $n = 6$), and soils (0.934, $p < 0.05$, $n = 4$) (Fig. 2), suggesting that inorganic Hg during this period may be highly bioavailable and is readily converted to MMHg. Accordingly, these floodplain lakes may therefore be important sites for MMHg bioaccumulation in fish, presenting a potential risk for human populations that depend on fish as their primary protein source (Brito et al. 2017).

Mercury isotope ratios

Variations in the isotopic composition of Hg in the sediments are likely due to a combination of different factors including different sources of Hg and the subsequent fractionation resulting from various physicochemical reactions in the water column and in sediments (Das et al. 2015). The lake and riverine sediments showed similar range of δ^{202}Hg values, suggesting a possible contribution of riverine Hg to floodplain lake sediments during the RW season (Fig. 3). As mentioned before, Hg associated with SPM plays a critical role in white water floodplain lakes. According to Chen et al. (2016), mercury transported by particles is also less reactive than Hg in the dissolved phase and thus, is more likely to preserve the source Hg isotope signatures (for both MDF and MIF).

The negative δ^{202}Hg values ($-1.40‰$ to $-0.89‰$) reported for the sediments of floodplain lakes are in the range reported for lake sediments elsewhere (δ^{202}Hg values

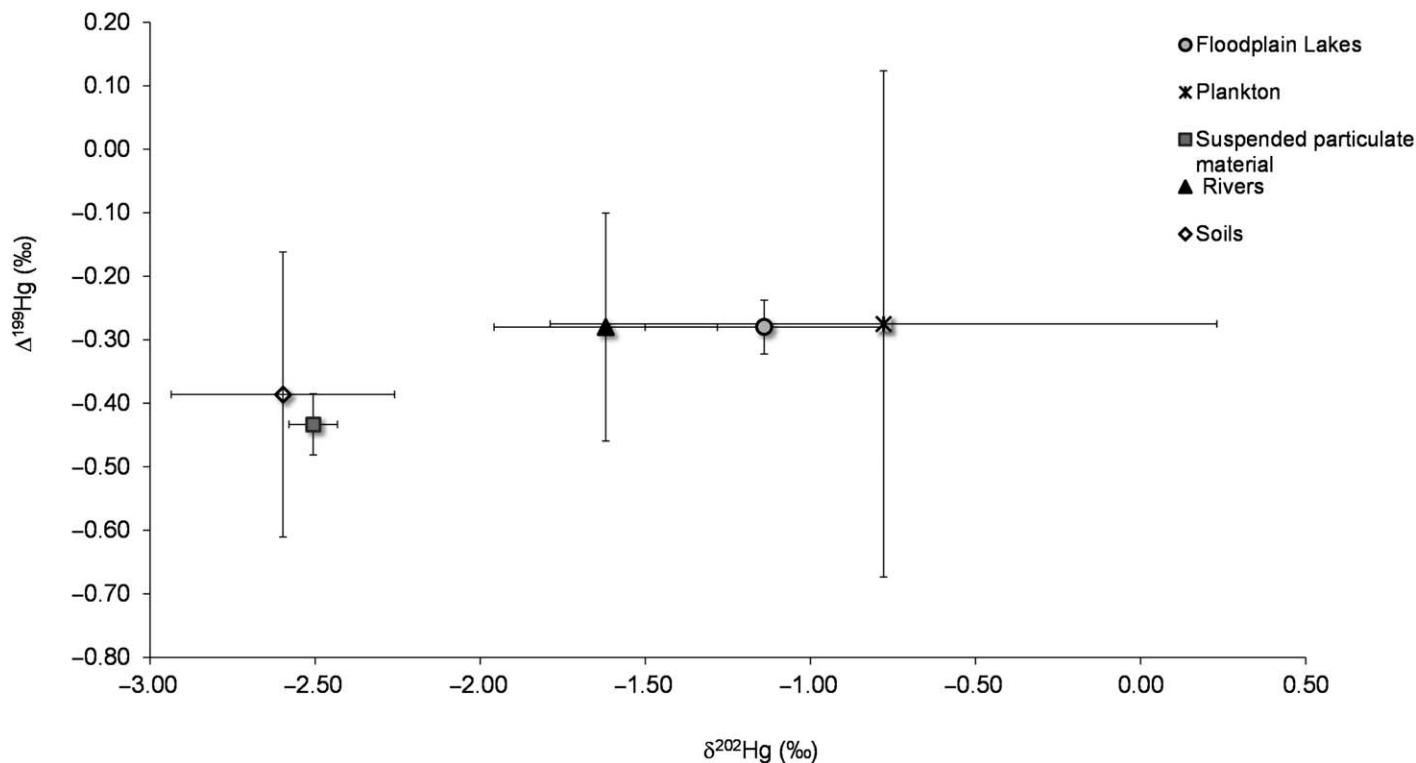**Fig. 3.** Relationship between δ^{202}Hg and Δ^{199}Hg in sediments, soils, and SPM from the Amazon Basin.

between 0‰ and −2.5‰, Blum et al. 2014). Jiskra et al. (2012) found preferential adsorption of light isotopes onto goethite resulting in a shift toward more negative δ^{202}Hg values on the solid (particulate) phase. Likewise, light Hg isotopes preferably also bind with thiol sites in OM (Wiederhold et al. 2010). Such processes could enrich light isotopes on particles or other OM and lead to an increase in Hg concentration and more negative δ^{202}Hg values for Hg associated with such materials. Our data would confirm such theories, showing significantly more negative δ^{202}Hg values and elevated THg concentrations in SPM (−2.60 ± 0.41‰, 779 ± 217 ng g^{-1}, respectively) compared to sediments (−1.14 ± 0.22‰, 86 ± 18 ng g^{-1}, respectively).

Other compartments frequently showing negative δ^{202}Hg values are tree foliage (Demers et al. 2013) and other plant derived environmental samples (Yin et al. 2013). Although the TOC concentration in sediment was not different in the study lakes, our data cannot exclude a difference in TOC quality. In fact, a recent study on organic biomarkers (lignin phenols) in similar samples highlighted the importance of OM input from vegetation to the floodplain lakes (Sobrinho et al. 2016) indicating that the quality of the OM may be influencing the transport by suspended particulate matter rich in lignin phenols. Moreover, Abril et al. (2014) found that the heterogeneity in the floodplains was related to the connections between the waters and vegetation at various spatial and temporal scales. Considering that Hg can

strongly bind to OM (Ravichandran 2004; Sanei and Goodarzi 2006), OM appears to be a key parameter to fully understand the dynamics of Hg transport in this ecosystem. Previous studies have also documented a relationship between quality of OM and Hg dynamics in different matrices (e.g., sediments, soils, and water column) (Caron et al. 2008; Teisserenc et al. 2010) through the association between lignin phenols and THg.

δ^{202}Hg values for SPM were similar to those found in soils (Table 3). Erosion has been reported as a main source for exporting Hg from the watershed (tributaries and rivers) to lakes (Lepak et al. 2015). In fact, some authors reported negative MDF and MIF values for forest soils ranging from −2.53‰ to −0.74‰ and from −0.58‰ to −0.14‰, respectively (Carignan et al. 2009; Demers et al. 2013; Blum et al. 2014). Moreover, mercury strongly bound to the soil matrix maybe subject to only minimal aqueous processing and therefore experiences negligible isotope fractionation during sedimentation (Foucher and Hintelmann 2009; Yin et al. 2016).

The Δ^{199}Hg values in lake sediments were consistently negative and did not differ significantly from those measured in other matrices ($p < 0.05$). Large MIF of odd Hg isotopes has previously been reported in precipitation and atmospheric Hg samples. For instance, Gratz et al. (2010) reported positive Δ^{199}Hg (from +0.04‰ to +0.52‰) in precipitation and negative Δ^{199}Hg (from −0.21‰ to +0.06‰) in gaseous Hg samples in the Great Lakes region (U.S.A.). Hg in

terrestrial soils is primarily a result of atmospheric Hg deposition and partial subsequent re-evasion, typically resulting in negative Δ^{199}Hg (Demers et al. 2013). Given that Δ^{199}Hg values in our investigated Amazon soils are also consistently negative, it would support our suggestion that watershed soil particles are the primary source of Hg to these lakes.

Previous laboratory studies of aqueous solutions with natural OM demonstrated that MIF is caused by photochemical reduction of Hg^{2+} and MMHg photodegradation to Hg^0 (Bergquist and Blum 2007). When Δ^{199}Hg vs. Δ^{201}Hg is plotted for the Hg remaining in solution, a slope of 1.36 is generally associated with MMHg photodemethylation and a slope of 1.00 with Hg^{2+} photoreduction processes (Bergquist and Blum 2007). The relationship between Δ^{199}Hg and Δ^{201}Hg for Hg in the floodplain lakes, soils, and rivers is characterized by a slope of 0.82, close to 1, which suggests that the observed MIF is associated with the dominance of inorganic Hg in these samples and most likely a result of photochemical reduction of Hg^{2+} (Supporting Information Material 2).

The Amazon forest has been widely recognized as a major component of the regional and global hydroclimate system, hosting the largest area of tropical rain forest and is considered as the prime contributor to land surface evapotranspiration. In addition to the significant influence on the global hydrological cycle, these sizable water fluxes are associated with energy fluxes that drive tropical convection and have a corresponding impact on global atmospheric circulation (Hasler and Avissar 2007). Consequently, we suggest that these hydrological processes must be considered to understand the Hg dynamics in the studied lakes. In addition, atmospheric Hg can be taken up by plant stomata (gaseous elemental Hg) and/or absorbed by leaf surfaces (particulate, reactive gaseous, and Hg in wet deposition). Subsequent throughfall, litterfall, or direct dry deposition moves Hg from the atmosphere to the forest (Lindberg et al. 1992). Forest canopies and soil regulate the magnitude and timing of the delivery of Hg to downstream aquatic ecosystems through these processes (Gong et al. 2014). Zocatelli et al. (2013) showed that the Amazon River transports OM adsorbed onto fine mineral particles to the Curuai Lake during periods of high water and establishes an effective connection to the main stream. Moreover, Hg can be re-emitted to the atmosphere and or can leach with dissolved organic matter into runoff or soil solution (Kocman et al. 2011). Thus, forests have a strong influence on regional Hg cycling.

References

Abril, G., and others. 2014. Amazon River carbon dioxide outgassing fuelled by wetlands. Nature **505**: 395–398. doi:10.1038/nature12797

Akagi, H., and A. Naganuma. 2000. Human exposure to mercury and the accumulation of methylmercury that is associated with gold mining in the Amazon Basin, Brazil. J. Health Sci. **46**: 323–328. doi:10.1248/jhs.46.323

Almeida, R. D., J. V. E. Bernardi, R. C. Oliveira, D. P. D. Carvalho, A. G. Manzatto, L. D. Lacerda, and W. R. Bastos. 2014. Flood pulse and spatial dynamics of mercury in sediments in Puruzinho lake, Brazilian Amazon. Acta Amaz. **44**: 99–105. doi:10.1590/S0044-59672014000100010

Balogh, S. J., M. T. K. Tsui, J. D. Blum, A. Matsuyama, G. E. Woerndle, S. Yano, and A. Tada. 2015. Tracking the fate of mercury in the fish and bottom sediments of Minamata Bay, Japan, using stable mercury isotopes. Environ. Sci. Technol. **49**: 5399–5406. doi:10.1021/acs.est.5b00631

Bergquist, B. A., and J. D. Blum. 2007. Mass-dependent and-independent fractionation of Hg isotopes by photoreduction in aquatic systems. Science **318**: 417–420. doi:10.1126/science.1148050

Bisinoti, M. C., and W. F. Jardim. 2004. O comportamento do metilmercúrio (metilHg) no ambiente. Quím. Nova **27**: 593–600. doi:10.1590/S0100-40422004000400014

Blum, J. D., and B. A. Bergquist. 2007. Reporting of variations in the natural isotopic composition of mercury. Anal. Bioanal. Chem. **388**: 353–359. doi:10.1007/s00216-007-1236-9

Blum, J. D., L. S. Sherman, and M. W. Johnson. 2014. Mercury isotopes in earth and environmental sciences. Annu. Rev. Earth Planet. Sci. **42**: 249–269. doi:10.1146/annurev-earth-050212-124107

Brito, B. C., B. R. Forsberg, D. Kasper, J. H. Amaral, M. R. de Vasconcelos, O. P. de Sousa, F. A. G. Cunha, and W. R. Bastos. 2017. The influence of inundation and lake morphometry on the dynamics of mercury in the water and plankton in an Amazon floodplain lake. Hydrobiologia **790**: 35–48. doi:10.1007/s10750-016-3017-y

Callede, J., P. Kosuth, J. L. Loup, and V. S. Guimarâes. 2000. Discharge determination by Acoustic Doppler Current Profilers (ADCP): A moving bottom error correction method and its application on the river Amazon at Obidos. Hydrol. Sci. J. **45**: 911–924. doi:10.1080/02626660009492392

Carignan, J., N. Estrade, J. E. Sonke, and O. F. Donard. 2009. Odd isotope deficits in atmospheric Hg measured in lichens. Environ. Sci. Technol. **43**: 5660–5664. doi:10.1021/es900578v

Caron, S., M. Lucotte, and R. Teisserenc. 2008. Mercury transfer from watersheds to aquatic environments following the erosion of agrarian soils: A molecular biomarker approach. Can. J. Soil Sci. **88**: 801–811. doi:10.4141/CJSS07112

Chen, J., H. Hintelmann, and B. Dimock. 2010. Chromatographic pre-concentration of Hg from dilute aqueous solutions for isotopic measurement by MC-ICP-MS. J. Anal. At. Spectrom. **25**: 1402–1409. doi:10.1039/c0ja00014k

Chen, J., H. Hintelmann, W. Zheng, X. Feng, H. Cai, Z. Wang, S. Yuan, and Z. Wang. 2016. Isotopic evidence for distinct sources of mercury in lake waters and sediments. Chemical Geology **426**: 33–44.

Das, R., W. Landing, M. Bizimis, L. Odom, and J. Caffrey. 2015. Mass independent fractionation of mercury isotopes as source tracers in sediments. Procedia Earth Planet. Sci. **13**: 151–157. doi:10.1016/j.proeps.2015.07.036

Demers, J. D., J. D. Blum, and D. R. Zak. 2013. Mercury isotopes in a forested ecosystem: Implications for air-surface exchange dynamics and the global mercury cycle. Global Biogeochem. Cycles **27**: 222–238. doi:10.1002/gbc.20021

Dunne, T., L. A. Mertes, R. H. Meade, J. E. Richey, and B. R. Forsberg. 1998. Exchanges of sediment between the flood plain and channel of the Amazon River in Brazil. Geol. Soc. Am. Bull. **110**: 450–467. doi:10.1130/0016-7606(1998)110<0450:EOSBTF>2.3.CO;2

Feng, X., D. Foucher, H. Hintelmann, H. Yan, T. He, and G. Qiu. 2010. Tracing mercury contamination sources in sediments using mercury isotope compositions. Environ. Sci. Technol. **44**: 3363–3368. doi:10.1021/es9039488

Fitzgerald, W. F., and T. W. Clarkson. 1991. Mercury and monomethylmercury: Present and future concerns. Environ. Health Perspect. **96**: 159–166. doi:10.1289/ehp.9196159

Forsberg, B. R., A. H. Devol, J. E. Richey, L. A. Martinelli, and H. Dos Santos. 1988. Factors controlling nutrient concentrations in Amazon floodplain lakes. Limnol. Oceanogr. **33**: 41–56. doi:10.4319/lo.1988.33.1.0041

Foucher, D., and H. Hintelmann. 2006. High-precision measurement of mercury isotope ratios in sediments using cold-vapor generation multi-collector inductively coupled plasma mass spectrometry. Anal. Bioanal. Chem. **384**: 1470–1478. doi:10.1007/s00216-006-0373-x

Foucher, D., and H. Hintelmann. 2009. Tracing mercury contamination from the Idrija mining region (Slovenia) to the Gulf of Trieste using Hg isotope ratio measurements. Environ. Sci. Technol. **43**: 33–39. doi:10.1021/es801772b

Gong, P., X. P. Wang, Y. G. Xue, B. Q. Xu, and T. D. Yao. 2014. Mercury distribution in the foliage and soil profiles of the Tibetan forest: Processes and implications for regional cycling. Environ. Pollut. **188**: 94–101. doi:10.1016/j.envpol.2014.01.020

Goulding, M., R. Barthem, and E. Ferreira. 2003. The Smithsonian Atlas of the Amazon. Smithsonian Institution.

Gratz, L., G. Keeler, J. D. Blum, and L. S. Sherman. 2010. Isotopic composition and fractionation of mercury in Great Lakes precipitation and ambient air. Environ. Sci. Technol. **44**: 7764–7770. doi:10.1021/es100383w

Guimarães, J. R. D., M. Meili, L. D. Hylander, E. D. C. Silva, M. Roulet, J. B. N. Mauro, and D. R A. Lemos. 2000. Mercury net methylation in five tropical flood plain regions of Brazil: High in the root zone of floating macrophyte mats but low in surface sediments and flooded soils. Sci. Total Environ. **261**: 99–107. doi:10.1016/S0048-9697(00)00628-8

Guyot, J. L., J. M. Jouanneau, L. Soares, G. R. Boaventura, N. Maillet, and C. Lagane. 2007. Clay mineral composition of river sediments in the Amazon Basin. Catena **71**: 340–356. doi:10.1016/j.catena.2007.02.002

Hacon, S., P. R. Barrocas, A.C.S.D. Vasconcellos, C. Barcellos, J. C. Wasserman, R. C. Campos, C. Ribeiro, and F. B. Azevedo-Carloni. 2008. An overview of mercury contamination research in the Amazon basin with an emphasis on Brazil. Cad. Saúde Publica **24**: 1479–1492. doi:10.1590/S0102-311X2008000700003

Hasler, N., and R. Avissar. 2007. What controls evapotranspiration in the Amazon basin? J. Hydrometeorol. **8**: 380–395. doi:10.1175/JHM587.1

Jackson, T. A., D. M. Whittle, M. S. Evans, and D. C. Muir. 2008. Evidence for mass-independent and mass-dependent fractionation of the stable isotopes of mercury by natural processes in aquatic ecosystems. Appl. Geochem. **23**: 547–571. doi:10.1016/j.apgeochem.2007.12.013

Jiskra, M., J. G. Wiederhold, B. Bourdon, and R. Kretzschmar. 2012. Solution speciation controls mercury isotope fractionation of Hg (II) sorption to goethite. Environ. Sci. Technol. **46**: 6654–6662. doi:10.1021/es3008112

Junk, W. J. 1997. General aspects of floodplain ecology with special reference to Amazonian floodplains, p. 3–20. *In* W. J. Junk [ed.], The central Amazon floodplain. Springer.

Junk, W. J., P. B. Bayley, and R. E. Sparks. 1989. The flood pulse concept in river-floodplain systems, p. 110–127. *In* D. P. Dodge [ed.], Proceedings of the International Large River Symposium (LARS). Canadian special publication of fisheries and aquatic sciences, v. 106. Department of Fisheries and Oceans.

Kocman, D., P. Vreča, V. Fajon, and M. Horvat. 2011. Atmospheric distribution and deposition of mercury in the Idrija Hg mine region, Slovenia. Environ. Res. **111**: 1–9. doi:10.1016/j.envres.2010.10.012

Lacerda, L. D. 1995. Amazon mercury emissions. Nature **374**: 21–22. doi:10.1038/374020a0

Lechler, P. J., J. R. Miller, L. D. Lacerda, D. Vinson, J. C. Bonzongo, W. B. Lyons, and J. J. Warwick. 2000. Elevated mercury concentrations in soils, sediments, water, and fish of the Madeira River basin, Brazilian Amazon: A function of natural enrichments. Sci. Total Environ. **260**: 87–96. doi:10.1016/S0048-9697(00)00543-X

Lepak, R. F., R. Yin, D. P. Krabbenhoft, J. M. Ogorek, J. F. DeWild, T. M. Holsen, and J. P. Hurley. 2015. Use of stable isotope signatures to determine mercury sources in the Great Lakes. Environ. Sci. Technol. Lett. **2**: 335–341. doi:10.1021/acs.estlett.5b00277

Lindberg, S., and others. 2007. A synthesis of progress and uncertainties in attributing the sources of mercury in deposition. Ambio **36**: 19–33. doi:10.1579/0044-7447(2007)36[19:ASOPAU]2.0.CO;2]

Lindberg, S. E., T. P. Meyers, G. E. Taylor, R. R. Turner, and W. H. Schroeder. 1992. Atmosphere-surface exchange of mercury in a forest: Results of modeling and gradient approaches. J. Geophys. Res. **97**: 2519–2528. doi:10.1029/91JD02831

Maia, P. D., L. Maurice, E. Tessier, D. Amouroux, D. Cossa, M. Pérez, P. Moreira-Turcq, and I. Rhéault. 2009. Mercury distribution and exchanges between the Amazon River and connected floodplain lakes. Sci. Total Environ. **407**: 6073–6084. doi:10.1016/j.scitotenv.2009.08.015

Malm, O. 1998. Gold mining as a source of mercury exposure in the Brazilian Amazon. Environ. Res. **77**: 73–78. doi:10.1006/enrs.1998.3828

Martinelli, L. A., R. L. Victoria, P. B. De Camargo, M. D. C. Piccolo, L. Mertes, J. E. Richey, A. H. Devol, and B. R. Forsberg. 2003. Inland variability of carbon–nitrogen concentrations and δ13C in Amazon floodplain (várzea) vegetation and sediment. Hydrol. Process. **17**: 1419–1430. doi:10.1002/hyp.1293

Meade, R. H., C. F. Nordin, W. F. Curtis, F. M. C. Rodrigues, C. M. Do Vale, and J. M. Edmond. 1979. Sediment loads in the Amazon River. Nature **278**: 161–163. doi:10.1038/278161a0

Melack, J. M. 1984. Amazon floodplain lakes: shape, fetch, and stratification. Verhandlungen des Internationalen Verein Limnologie **22**: 1278–1281.

Melack, J. M., and T. R. Fisher. 1990. Comparative limnology of tropical floodplain lakes with an emphasis on the central Amazon. Acta Limnol. Bras. **3**: 1–48.

Mertes, L. A., D. L. Daniel, J. M. Melack, B. Nelson, L. A. Martinelli, and B. R. Forsberg. 1995. Spatial patterns of hydrology, geomorphology, and vegetation on the floodplain of the Amazon River in Brazil from a remote sensing perspective. Geomorphology **13**: 215–232. doi:10.1016/0169-555X(95)00038-7

Morel, F. M., A. M. Kraepiel, and M. Amyot. 1998. The chemical cycle and bioaccumulation of mercury. Annu. Rev. Ecol. Syst. **29**: 543–566. doi:10.1146/annurev.ecolsys.29.1.543

Oestreicher, J. S., M. Lucotte, M. Moingt, É. Bélanger, C. Rozon, R. Davidson, F. Mertens, and C. A. Romaña. 2017. Environmental and anthropogenic factors influencing mercury dynamics during the past century in floodplain lakes of the Tapajós River, Brazilian Amazon. Arch. Environ. Contam. Toxicol. **72**: 11–30. doi:10.1007/s00244-016-0325-1

Perrot, V., and others. 2010. Tracing sources and bioaccumulation of mercury in fish of Lake Baikal− Angara River using Hg isotopic composition. Environ. Sci. Technol. **44**: 8030–8037. doi:10.1021/es101898e

Pfeiffer, W. C., L. D. Lacerda, W. Salomons, and O. Malm. 1993. Environmental fate of mercury from gold mining in the Brazilian Amazon. Environ. Rev. **1**: 26–37. doi:10.1139/a93-004

Ravichandran, M. 2004. Interactions between mercury and dissolved organic matter—a review. Chemosphere **55**: 319–331. doi:10.1016/j.chemosphere.2003.11.011

Rolison, J. M., W. M. Landing, W. Luke, M. Cohen, and V. J. M. Salters. 2013. Isotopic composition of species-specific atmospheric Hg in a coastal environment. Chem. Geol. **336**: 37–49. doi:10.1016/j.chemgeo.2012.10.007

Roulet, M., and M. Lucotte. 1995. Geochemistry of mercury in pristine and flooded ferralitic soils of a tropical rain forest in French Guiana, South America, p. 1079–1088. *In* D. B. Porcella, J. W. Huckabee, and B. Wheatley [eds.], Mercury as a global pollutant. Springer.

Roulet, M., M. Lucotte, A. Saint-Aubin, S. Tran, I. Rheault, N. Farella, and D. Mergler. 1998*a*. The geochemistry of mercury in central Amazonian soils developed on the Alter-do-Chao formation of the lower Tapajos River Valley, Para state, Brazil. Sci. Total Environ. **223**: 1–24. doi:10.1016/S0048-9697(98)00265-4

Roulet, M., M. Lucotte, N. Farella, G. Serique, H. Coelho, C. S. Passos, and M. Amorim. 1998*b*. Effects of recent human colonization on the presence of mercury in Amazonian ecosystems. Water Air Soil Poll. **112**: 297–313. doi:10.1023/A:1005073432015

Roulet, M., and others. 1998*c*. Distribution and partition of total mercury in waters of the Tapajós River Basin, Brazilian Amazon. Sci. Total Environ. **213**: 203–211. doi:10.1016/S0048-9697(98)00093-X

Roulet, M., and others. 1999. Effects of recent human colonization on the presence of mercury in Amazonian ecosystems. Water Air Soil Pollut. **112**: 297–313. doi:10.1023/A:1005073432015

Roulet, M., and others. 2001. Spatio-temporal geochemistry of mercury in waters of the Tapajós and Amazon Rivers, Brazil. Limnol. Oceanogr. **46**: 1141–1157. doi:10.4319/lo.2001.46.5.1141

Run-Sheng, Y. I. N., F. E. N. G. Xin-Bin, D. Foucher, S. H. I. Wen-Fang, Z. H. A. O. Zhi-Qi, and W. A. N. G. Jing 2010. High precision determination of mercury isotope ratios using online mercury vapor generation system coupled with multicollector inductively coupled plasma-mass spectrometer. Chinese Journal of Analytical Chemistry **38**: 929–934.

Salati, E., and P. B. Vose. 1984. Amazon basin: A system in equilibrium. Science **225**: 129–138. doi:10.1126/science.225.4658.129

Sanei, H., and F. Goodarzi. 2006. Relationship between organic matter and mercury in recent lake sediment: The physical–geochemical aspects. Appl. Geochem. **21**: 1900–1912. doi:10.1016/j.apgeochem.2006.08.015

Sherman, L. S., and J. D. Blum. 2013. Mercury stable isotopes in sediments and largemouth bass from Florida lakes, USA. Sci. Total Environ. **448**: 163–175. doi:10.1016/j.scitotenv.2012.09.038

Silva, G. S. D., M. C. Bisinoti, P. S. Fadini, G. Magarelli, W. F. Jardim, and A. H. Fostier. 2009. Major aspects of the mercury cycle in the Negro River Basin, Amazon. J. Braz. Chem. Soc. **20**: 1127–1134. doi:10.1590/S0103-50532009000600019

Sioli, H. [ed.]. 1984. The Amazon: Limnology and landscape ecology of a mighty tropical river and its basin, p. 216–243. Dr. W.J. Junk Publishers.

Sobrinho, R. L., and others. 2016. Spatial and seasonal contrasts of sedimentary organic matter in floodplain lakes of the central Amazon basin. Biogeosciences **13**: 467–482. doi:10.5194/bg-13-467-2016

Sonke, J. E., J. Schäfer, J. Chmeleff, S. Audry, G. Blanc, and B. Dupré. 2010. Sedimentary mercury stable isotope records of atmospheric and riverine pollution from two major European heavy metal refineries. Chem. Geol. **279**: 90–100. doi:10.1016/j.chemgeo.2010.09.017

Teisserenc, R., M. Lucotte, and S. Houel. 2010. Terrestrial organic matter biomarkers as tracers of Hg sources in lake sediments. Biogeochemistry **103**: 235. doi:10.1007/s10533-010-9458-x

Tsui, M. T., and W. X. Wang. 2004. Uptake and elimination routes of inorganic mercury and methylmercury in *Daphnia magna*. Environ. Sci. Technol. **38**: 808–816. doi:10.1021/es034638x

Ullrich, S. M., T. W. Tanton, and S. A. Abdrashitova. 2001. Mercury in the aquatic environment: A review of factors affecting methylation. Crit. Rev. Environ. Sci. Technol. **31**: 241–293. doi:10.1080/20016491089226

U.S. EPA. Method 1630. 1998. Methyl mercury in water by distillation, aqueous ethylation, purge and trap, and CVAFS. US Environmental Protection Agency.

U.S. EPA. Method 1631. 1999. Mercury in water by oxidation, purge and trap, and cold vapor atomic fluorescence spectrometry. U.S. EPA 821-R-95-027. Office of Water, Engineering and Analysis Division (4303).

Victoria, R. L., L. A. Martinelli, P. C. Trivelin, E. Matsui, B. R. Forsberg, J. E. Richey, and A. H. Devol. 1992. The use of stable isotopes in studies of nutrient cycling: Carbon isotope composition of Amazon varzea sediments. Biotropica **24**: 240–249. doi:10.2307/2388518

Wasserman, J. C., S. Hacon, and M. A. Wasserman. 2003. Biogeochemistry of mercury in the Amazonian environment. Ambio **32**: 336–342. doi:10.1579/0044-7447-32.5.336

Wiederhold, J. G., C. J. Cramer, K. Daniel, I. Infante, B. Bourdon, and R. Kretzschmar. 2010. Equilibrium mercury isotope fractionation between dissolved Hg (II) species and thiol-bound Hg. Environ. Sci. Technol. **44**: 4191–4197. doi:10.1021/es100205t

Yin, R., and others. 2013. Mercury speciation and mercury isotope fractionation during ore roasting process and their implication to source identification of downstream sediment in the Wanshan mercury mining area, SW China. Chem. Geol. **336**: 72–79. doi:10.1016/j.chemgeo.2012.04.030

Yin, R., X. Feng, X. Li, B. Yu, and B. Du. 2014. Trends and advances in mercury stable isotopes as a geochemical tracer. Trends Environ. Anal. Chem. **2**: 1–10. doi:10.1016/j.teac.2014.03.001

Yin, R., X. Feng, B. Chen, J. Zhang, W. Wang, and X. Li. 2015. Identifying the sources and processes of mercury in subtropical estuarine and ocean sediments using Hg isotopic composition. Environ. Sci. Technol. **49**: 1347–1355. doi:10.1021/es504070y

Yin, R., R. F. Lepak, D. P. Krabbenhoft, and J. P. Hurley. 2016. Sedimentary records of mercury stable isotopes in Lake Michigan. Elem. Sci Anth. **4**: 000086. doi:10.12952/journal.elementa.000086

Zheng, W., Z. Xie, and B. A. Bergquist. 2015. Mercury stable isotopes in ornithogenic deposits as tracers of historical cycling of mercury in Ross Sea, Antarctica. Environ. Sci. Technol. **49**: 7623–7632. doi:10.1021/acs.est.5b00523

Zocatelli, R., P. Moreira-Turcq, M. C. Bernardes, B. Turcq, R. C. Cordeiro, S. Gogo, J. R. Disnar, and M. Boussafir. 2013. Sedimentary evidence of soil organic matter input to the Curuai Amazonian floodplain. Org. Geochem. **63**: 40–47. doi:10.1016/j.orggeochem.2013.08.004

Conflict of Interest
None declared.